Mon. Not. R. Astron. Soc. **000**, 000–000 (0000) Printed 7 June 2001 (MN LaTeX style file v2.2)

The magnetic field and wind confinement of β Cephei: new clues for interpreting the Be phenomenon?

J.-F. Donati[1], G.A. Wade[2], J. Babel[3], H.F. Henrichs[4], J.A. de Jong[4], T.J. Harries[5]

[1] *Laboratoire d'Astrophysique, Observatoire Midi-Pyrénées, 14 Av. E. Belin, F–31400 Toulouse, France (*`donati@obs-mip.fr`*)*
[2] *Dépt. de Physique, Université de Montréal, CP 6128 succ Centre-Ville, Montréal QC, Canada H3C 3J7 (*`wade@astro.umontreal.ca`*)*
[3] *36 rue des Battieux, 2000 Neuchatel, Switzerland (*`babeljr@bluewin.ch`*)*
[4] *Astronomical Institute 'Anton Pannekoek', University of Amsterdam, Kruislaan 403, 1098SJ Amsterdam, Netherlands (*`huib@astro.uva.nl, jdj@astro.uva.nl`*)*
[5] *School of Physics, University of Exeter, Stocker Road, Exeter EX4 4QL, UK (*`th@astro.ex.ac.uk`*)*

2000, MNRAS, submitted

ABSTRACT

In this paper, we use the very recent spectropolarimetric observations of β Cep collected by Henrichs et al. (2001) and propose for this star a consistent model of the large scale magnetic field and of the associated magnetically confined wind and circumstellar environment. A re-examination of the fundamental parameters of β Cep in the light of the Hipparcos parallax indicates that this star is most likely a 12 $M_\odot$ star with a radius of 7 $R_\odot$, effective temperature of 26000 K and age of 12 Myr, viewed with an inclination of the rotation axis of about 60°. Using two different modelling strategies, we obtain that the magnetic field of β Cep can be approximately described as a dipole with a polar strength of 360 ± 30 G, whose axis of symmetry is tilted with respect to the rotation axis by about $85° \pm 10°$.

Although one of the weakest detected to date, this magnetic field is strong enough to confine magnetically the wind of β Cep up to a distance of about 8 to 9 R_*. We find that both the X-ray luminosity and variability of β Cep can be explained within the framework of the magnetically confined wind shock model of Babel & Montmerle (1997a), in which the stellar wind streams from both magnetic hemispheres collide with each other in the magnetic equatorial plane, producing a strong shock, an extended postshock region and a high density cooling disc.

By studying the stability of the cooling disc, we obtain that field lines can support the increasing disc weight for no more than a month before they become significantly elongated to equilibrate the gravitational plus centrifugal force, thereby generating strong field gradients across the disc. The associated current sheet eventually tears, forcing the field to reconnect through resistive diffusion and the disc plasma to collapse towards the star. We propose that this collapse is the cause for the recurrent Be episodes of β Cep, and finally discuss the applicability of this model to He peculiar, classical Be and normal non-supergiant B stars.

Key words: Stars: magnetic fields – winds – Be – B – rotation – pulsation

1 INTRODUCTION

As the prototype of the β Cep class of pulsating stars, β Cep (HD 205021, spectral type B1 IV) has been studied extensively for its short term multiperiodic photometric and photospheric line profile variability (e.g. Heynderickx et al. 1994; Telting et al. 1997; Shibahashi & Aerts 2000). In addition to these phenomena, β Cep also exhibits large amplitude, longer-term, periodic time variations of the equivalent width of ultraviolet resonance lines (Fishel & Sparks 1972; Henrichs et al. 1993, 1998, 2001; Smith & Groote 2001) with a remarkably stable phase dependence over long intervals. This behaviour is strikingly similar to that of most well-studied chemically peculiar magnetic B stars (e.g. Barker et al. 1982; Wade et al. 1997), for which this variability is commonly interpreted as rotational modulation of a dense magnetosphere tilted with respect to the stellar rotation axis (e.g. Shore & Brown 1990; Babel & Montmerle 1997a).

The idea that the same scheme may apply for β Cep, i.e. that it also hosts an oblique magnetic field and thus a dense magnetosphere, is very natural, and may yield some insights into the recurrent Be episodes that this star undergoes every few decades, the latest recorded event being dated from early 1990 (Mathias et al. 1991). It could also provide a natural explanation of the X-ray emission this star exhibits (along with other near-main sequence early B/Be stars, e.g. Berghöfer et al. 1996), and which cannot be accounted for by the self-excited wind instability mechanism usually invoked for hot stars (e.g. Cohen et al. 2001).

The first attempt at detecting magnetic fields on β Cep was performed by Rudy & Kemp (1978), using a photoelectric Pockels cell polarimeter measuring circular polarisation in the wings of one Balmer line (e.g. Landstreet 1982) and thus the line-of-sight projected component of the magnetic field averaged over the stellar disc (hereafter referred to as the longitudinal field). They reported only a marginally significant result (longitudinal field of order 1 kG), with only one of their nine measurements exceeding the 3σ threshold. More than a decade later, Henrichs et al. (1993) secured new observations of β Cep using a similar polarimeter at the 1.2 m telescope of University of Western Ontario. Although much more precise than in the previous experiment (with error bars on the longitudinal field as low as 150 G), these new observations could not confirm the presence of magnetic fields on β Cep, casting at the same time serious doubts on the reality of Rudy & Kemp's (1978) earlier claim.

Very recently, a third attempt was carried out by Henrichs et al. (2001), using new high resolution spectropolarimetry. As discussed by Henrichs et al. (2001), the magnetic field of β Cep is clearly detected, and their preliminary analysis concludes that the magnetic field resembles a dipole with a polar field strength of order 300 G. The longitudinal field of β Cep is found to vary (and change sign) with the same period as the equivalent width of UV resonance lines (e.g. C IV, traditionally used as a stellar wind probe), confirming that this period (12.00092 d) is indeed the rotation period of the star, as suggested earlier by Henrichs et al. (1993, 1998). In particular, Henrichs et al. obtain that phases of longitudinal field extrema coincide with phases of maximum emission in the UV stellar wind lines (and thus minimum absorption by the wind and circumstellar plasma), further strengthening the observational similarity with He peculiar stars (e.g. Shore & Brown 1990).

In this paper, we present a more detailed analysis, modelling and interpretation of the magnetic data presented by Henrichs et al. (2001). After deriving an updated set of fundamental parameters for β Cep from the most recent papers published on this star in the literature (Sect. 2), we describe two different ways of modelling the magnetic field of β Cep, from analysing the observed variability of either the longitudinal field values or of the Stokes V profiles (Sect. 3). We then study extensively (in Sects. 4 and 5) the impact of this magnetic field on the wind and circumstellar environment of β Cep within the framework of the magnetically confined wind shock model of Babel & Montmerle (1997a, b), and suggest (in Sect. 6) that our new model may be relevant to other stellar classes such as main sequence chemically peculiar stars, Be stars and normal B stars.

2 STELLAR PARAMETERS

Before beginning construction of a new model for the magnetic field and circumstellar environment of β Cep, it is important to obtain as accurate fundamental parameters as possible, for both the star itself and the host binary system. With this aim, we scanned all relevant literature published to date.

2.1 Evolutionary status and wind parameters

From its visual magnitude ($m_{\rm V}$ = 3.2), effective temperature ($T_{\rm eff}$ = 26000 ± 1000 K, Gies & Lambert 1992), Hipparcos distance (182 ± 18 pc) and extinction coefficient ($A_{\rm V}$ = 0.1, Zorec & Briot 1991), we conclude that β Cep has a bolometric magnitude of -5.8 ± 0.2 (using a bolometric correction of –2.6, Bessel et al. 1998) and is thus 4.22 ± 0.08 dex more luminous than the Sun, with a radius of $R_* = 6.5 \pm 1.2$ $R_\odot$. This radius estimate implies an apparent diameter of about 0.32 mas, in reasonable agreement with the actual measurements mentioned in Underhill et al. (1979) and Remie & Lamers (1982). At the same time, the line-of-sight projected equatorial rotation velocity of β Cep (equal to $v \sin i = 27 \pm 2$ km s^{-1}, Telting et al. 1997) along with the rotation period of 12.00092 d (Henrichs et al. 2001) yields a line-of-sight projected radius $R_* \sin i$ of 6.4 ± 0.5 $R_\odot$ (in good agreement with the previous estimate), indicating that the inclination angle of β Cep lies between 50° and 90°. From a comparison of its location in the HR diagram with the evolutionary tracks for solar metalicity of Schaller et al. (1992), we obtain that β Cep has a mass of 12 ± 1 $M_\odot$ and an age of about 12 Myr. Thus our best estimate is that β Cep is a 12 $M_\odot$ star with a 7 $R_\odot$ radius viewed at an inclination angle of about 60°. Some of these parameters, and in particular the effective temperature, the radius and thus the luminosity, are known to be modulated by the radial pulsation. Maximum luminosity (+8.8% with respect to the mean) is attained when β Cep reaches minimum radius (–1.1%, determined from the radial pulsation velocity of Telting et al. 1997 and the above radius estimate) and maximum temperature (+2.7%, Beeckmans & Burger 1977).

This stellar model is consistent with the identification of the main pulsation period as the radial fundamental mode; the position of β Cep in the HR diagram indeed falls exactly on the intersection of the full line in Fig. 2 of Shibahashi & Aerts (2000, joining all stellar models whose fundamental pulsation period is 0.1904852 d) and the 12 $M_\odot$ star evolutionary track of Schaller et al. (1992, slightly brighter and hotter than the corresponding track in the older models of Pacynski 1970 used by Shibahashi & Aerts 2000). A quick look at the same Fig. 2 of Shibahashi & Aerts (2000) seems to invalidate the identification of the second strongest peak in the pulsation periodogram as an $\ell = 2$ mode (which would apparently require the star to have an effective temperature and/or luminosity inconsistent with the observed values). However, it appears that the dashed tracks in Shibahashi & Aerts's (2000) Fig. 2 (indicating the locus of stellar models that can potentially pulsate on this mode with the observed frequency) are incompatible with their own Fig. 1 (e.g. the dashed line labelled '$\ell = 2$ f' crosses the 10 $M_\odot$ star track only once in Fig. 2 while it should cross it four times according to Fig. 1), implying that their analysis is thus at least partly incorrect. Note that it is not clear either why these authors did not consider the other possible identification of this mode ($\ell = m = 1$) originally suggested by Telting et al. (1997).

There is no direct measurement of the main wind parameters (i.e. mass loss rate and maximum wind velocity) available in the literature for β Cep. We must therefore estimate these parameters based on measurements of normal non-supergiant B stars of similar spectral type, using for instance the survey of Prinja (1989). We first obtain that β Cep should have a terminal velocity of the order of the escape velocity (equal to 800 $\mathrm{km\,s^{-1}}$ in the case of β Cep). This is in reasonable agreement with observations of the C IV line profile, showing variability down to velocities of –750 $\mathrm{km\,s^{-1}}$ (Henrichs et al. 2001) and with the theoretical estimates of Abbott (1982, using the CAK theory of stellar winds) predicting a terminal velocity 10% smaller than the escape velocity for a star like β Cep. Since both the observational and theoretical values are known to underestimate the true terminal velocity (e.g. Abbott 1982), we used for β Cep a value of 900 $\mathrm{km\,s^{-1}}$ in the following. We also read from Prinja (1989) that the sum of the logarithmic mass loss rate (expressed in $M_\odot\,\mathrm{yr^{-1}}$) and the logarithmic C IV ionisation fraction should equal about –12. Assuming a logarithmic C IV ionisation fraction of –3 (typical for O and early B stars), we obtain a mass loss rate of about 10^{-9} $M_\odot\,\mathrm{yr^{-1}}$. Given the rather poor accuracy (not better than a factor of 3), this estimate is found to agree reasonably well with the empirical relationship between mass loss rate and luminosity of hot stars (predicting a value of 4×10^{-9} $M_\odot\,\mathrm{yr^{-1}}$ for β Cep) derived by Abbott (1982) from a fit to radio and UV observations. We thus believe that the derived value is more appropriate than that predicted by the CAK model for a star like β Cep (2.4×10^{-8} $M_\odot\,\mathrm{yr^{-1}}$, Abbott 1982). Note that we also expect the wind parameters to be modulated by the radial pulsation. Assuming that the mass loss rate is proportional to the square of the stellar luminosity (e.g. Abbott 1982), we estimate that the mass loss rate of β Cep should be modulated by about ±18% in response to the ±8.8% pulsation-induced luminosity changes, while the terminal velocity should remain roughly constant.

As already mentioned in the introduction, another parameter of interest in the context of wind models is the X-ray luminosity. The latest measurements with the ROSAT X-ray satellite give an X-ray luminosity of 0.5 to 1.0×10^{31} $\mathrm{erg\,s^{-1}}$ (Berghöfer et al. 1996; Cohen et al. 2001), depending on the exact methods of extracting counts from ROSAT images and estimating the total luminosity from a given ROSAT spectrum. It corresponds to a logarithmic $L_\mathrm{X}/L_\mathrm{bol}$ luminosity ratio of about –7, typical for early B stars (Cohen et al. 1997). The X-ray radiation of β Cep is rather soft (like for other β Cep stars, Cohen et al. 2001), with a temperature of about 0.24 keV (or 2.8 MK) and an emission measure of $2-5 \times 10^{53}$ $\mathrm{cm^{-3}}$. Worth noting is the recent discovery that the X-ray luminosity is modulated by the radial pulsation, with an amplitude of about ±6.7% (Cohen et al. 2001). No evidence yet exists for any variability of the X-ray luminosity with the rotation of the star.

2.2 Orbital parameters

Pigulski & Boratyn (1992) demonstrated that the apparent long-term fluctuations in the pulsation period and in the mean radial velocity of β Cep can be understood in terms of orbital motion of the variable star in a binary system, in which the secondary is the less massive companion detected by speckle interferometry (Gezari et al. 1972).

From Henrichs et al. (2001), we know that β Cep reached maximum radial velocity at pulsation phase 0.36 ± 0.01 (using the ephemeris of Pigulski & Boratyn 1992, in which maximum radial velocity should occur at phase 0.0 if β Cep was single), i.e. 0.112 ± 0.002 d ahead of the time predicted by the ephemeris. From Figs. 1 and 4 of Pigulski & Boratyn (1992), we obtain that these observations were recorded when β Cep was very close to periastron and thus that the orbital period of the system is 85 ± 1 yr, slightly shorter than (though still roughly compatible with) the value of 91.6 ± 3.7 derived by Pigulski & Boratyn (1992). With this value of the orbital period, the major semi-axis of the variable star orbit becomes 17.2 ± 1.0 AU and the mass function 0.72 ± 0.10 $M_\odot$.

Even though the distance of β Cep is now known with reasonable accuracy, the uncertainty on the major semi-axis of the true orbit (whose estimate from speckle interferometry measurements is $0.25 \pm 0.07''$ or 46 ± 14 AU for a distance of 182 ± 18 pc) is still too large to constrain usefully the mass of both system components. Until new interferometric measurements of β Cep close to periastron are available in the literature, we can only verify that the mass we obtain in Sect. 2.1, implying a major semi-axis of the true orbit of 50 ± 2 AU or $0.28 \pm 0.01''$, is compatible with the observations.

In this context, we find that the companion of β Cep has a mass of 6.2 ± 0.3 $M_\odot$, a logarithmic bolometric luminosity (with respect to the Sun) of 3.11 and a temperature of 19000 K. The corresponding bolometric magnitude contrast between components is 2.8 mag, while that for the B and V photometric bands reduces to about 2.3 mag. Unfortunately, this parameter cannot be used to validate our modelling, as estimates from speckle interferometry found in the literature are rather discrepant (ranging from up to 5 mag according to Gezari et al. 1972 down to less than 2 magnitudes according to Bonneau et al. 1980) and are thus likely unreliable.

3 MAGNETIC MODELLING

3.1 Mean Zeeman signatures and longitudinal field estimates

The data set we use in this paper consists of the 23 circularly polarised (Stokes V) and unpolarised (Stokes I) spectra secured by Henrichs et al. (2001) between 1998 December and 1999 July, using the MuSiCoS spectropolarimeter (Donati et al. 1999) mounted on the 2 m Télescope Bernard Lyot (TBL) at the Observatoire du Pic du Midi. These spectra, processed with a dedicated reduction package, ESpRIT (Donati et al. 1997), cover the spectral range 450–660 nm with a resolving power of about 35,000. For all other specific details about the observations, the reader is referred to Henrichs et al. (2001).

Mean Zeeman signatures were inferred using Least Square Deconvolution (LSD, Donati et al. 1997), a new cross-correlation type technique that enables the extraction of the polarisation information from all photospheric spectral lines in the observed wavelength range. The line list we employed for LSD (identical to that of Henrichs et al.

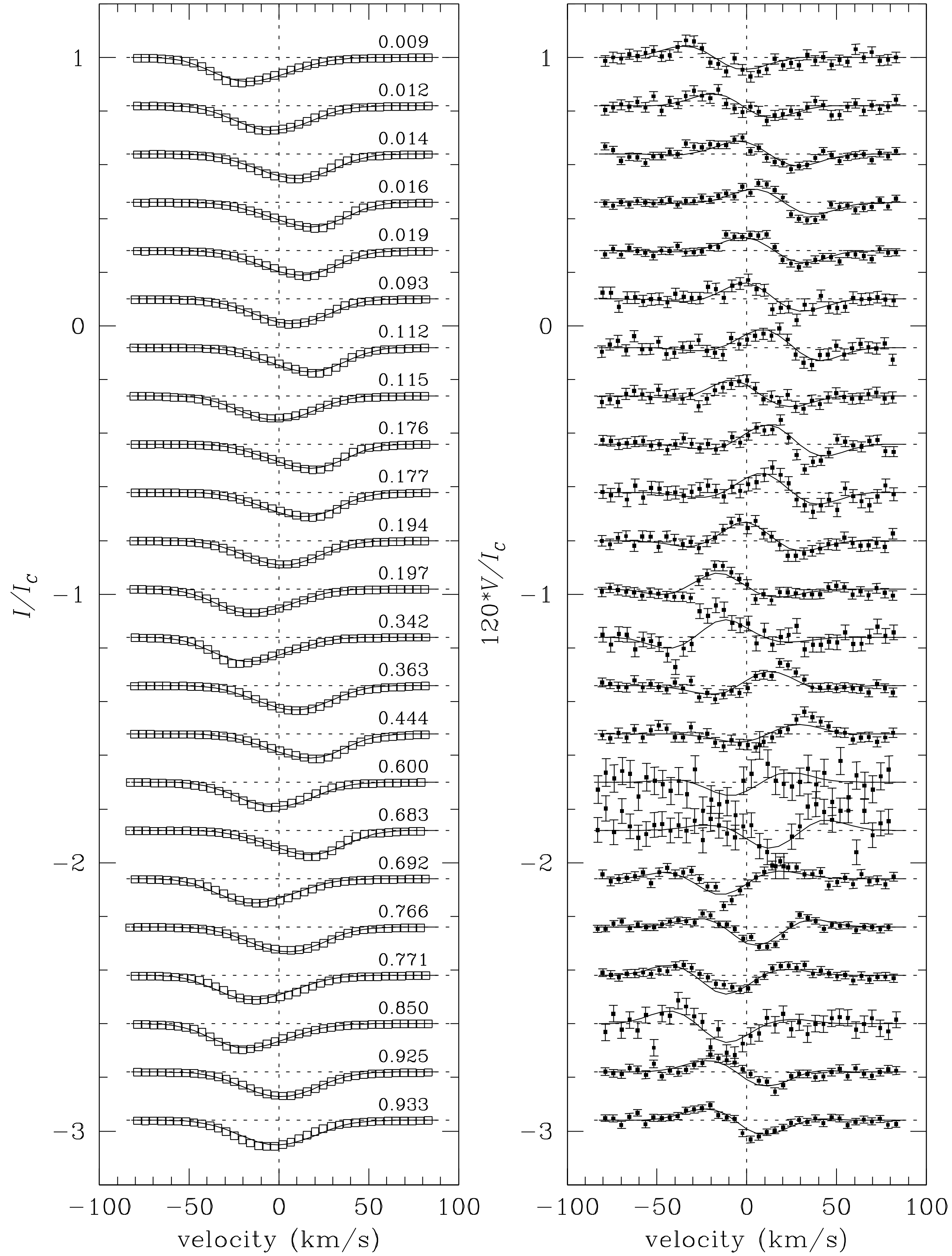

Figure 1. Least squares deconvolved Stokes I (left) and V (right) profiles of β Cep, derived from the spectra of Henrichs et al. (2001). The symbols represent the data (and error bars in the case of the Stokes V profiles) while the full line depicts the best fit with a tilted dipole model. Rotational phases (indicated above each LSD Stokes I profile) are computed with the ephemeris of Henrichs et al. ($\mathrm{JD} = 2,451,238.15 + 12.00092 \times E$). Note that all profiles are shifted vertically and that Stokes V signatures are expanded by a factor of 120 for display purposes.

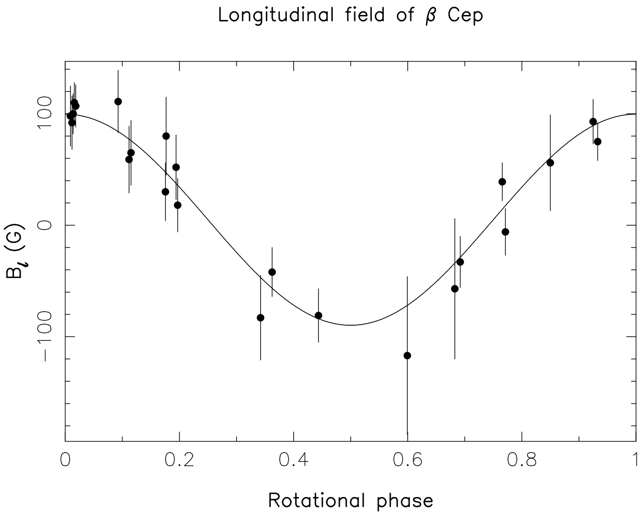

Figure 2. Longitudinal field estimates (filled circles) and error bars derived from the LSD Stokes profiles of Fig. 1, as a function of rotational phase (assuming a rotation period of 12.00092 d and defining phase 0.0 as the phase of longitudinal field maximum). The full line depicts the least-squares cosine fit to the data.

2001) was computed specifically for β Cep from a $\log g = 4$ and $T_{\rm eff} = 26000$ K LTE Atlas9 model atmosphere (Kurucz 1993). Note that we ensured that all spectral lines whose relative depth in the observed spectrum exceeds 10% of the continuum level are present in the list; we also removed from the list the very few predicted lines that do not appear in the spectra. Altogether, 127 occurrences of 79 spectral lines are used to derive the final LSD profiles, shown in Fig. 1. While the most obvious variability in both Stokes I and Stokes V is that induced by the fundamental radial pulsation mode of β Cep, one can nevertheless see quite clearly the superimposed rotational modulation of the Stokes V signature (and in particular the associated sign switch of the magnetic signal around phase 0.25 and 0.75).

Very accurate longitudinal field estimates B_ℓ can be easily obtained by measuring the first moment of the Stokes V profile (normalised by the line equivalent width), as detailed by Donati et al. (1997) and Wade et al. (2000). The B_ℓ values and error bars we derive (see Fig. 2) are in perfect agreement with those of Henrichs et al. (2001) and can be fitted to within their formal errors (reduced χ^2 of 0.5) by a cosine function with a fixed period of 12.00092 d, yielding a longitudinal field semi amplitude $B_{\max}$ of 95 ± 8 G about a mean value B_0 of 5 ± 6 G. The corresponding ephemeris for the epoch of longitudinal field maximum (as obtained by Henrichs et al. 2001 and confirmed by our cosine fit) is:

$$\mathrm{JD} = 2,451,238.15 \pm 0.15 + 12.00092 \times E,$$

where E denotes the number of cycles. We emphasise that these B_ℓ data are completely *incompatible* with a rotation period of order 6 d, which yields a totally incoherent B_ℓ versus phase relation (with very different B_ℓ values at very similar phases) and an associated reduced χ^2 in excess of 3. This implies in particular that all internal structure or atmospheric models of β Cep derived under the assumption of a 6 d rotation period (e.g. Shibahashi & Aerts 2000) can be considered as invalid.

The most natural explanation for the sinusoidal time variation of the longitudinal field detected on β Cep is that this star hosts a rather simple, approximately dipolar, large scale magnetic field whose axis of symmetry is tilted with respect to the rotation axis (the oblique rotator model). We thus assume in the following that the magnetic field is a tilted dipole, described by its polar strength $B_{\rm p}$ and its obliquity angle β with respect to the rotation axis. We have employed two different strategies to determine the values of these parameters.

3.2 Modelling the longitudinal field curve

The first way to proceed is to model the longitudinal field phase dependence shown in Fig. 2. For a tilted dipole, the variation of B_ℓ with rotation phase ϕ is given by Preston's (1967) well-known relation:

$$B_\ell = B_{\rm p}\,\frac{15+u}{20(3-u)}\left(\cos\beta\cos i + \sin\beta\sin i\cos 2\pi(\phi-\phi_0)\right),$$

where u denotes the limb darkening parameter and ϕ_0 the phase of longitudinal field maximum (equal to $u = 0.33$ and $\phi_0 = 0.0$ in the particular case of β Cep). From the fact that the B_ℓ data vary almost symmetrically about 0 (see Sect. 3.1), we straightforwardly obtain that either i or β (or both) are close to 90°. More quantitative estimates of i and β can be derived by measuring the ratio of longitudinal field maximum to longitudinal field minimum, equal to $\cos(\beta - i)/\cos(\beta+i)$ in the previous formula. The sine fit to our B_ℓ data indicates that this ratio is -1.11 ± 0.18, and thus that $\beta = 85° \pm 10°$ if we assume $i = 60°$. As i increases, β becomes progressively less constrained and can eventually take any value when i reaches 90°. Similarly, we find that $B_{\rm p}$ is well determined at a value of 375 ± 30 G for $i = 60°$; when i gets closer to 90°, $B_{\rm p}$ can no longer be estimated independently from β and only obeys $B_{\rm p}\ \sin\beta = 325 \pm 30$ G.

The longitudinal field data are rather noisy and sparsely sampled, and it is not yet possible to identify reliably small potential departures of the magnetic field of β Cep from a dipolar configuration.

3.3 Modelling the Stokes V profiles

The second method consists in modelling the Stokes V profiles to determine how well they can be fitted under the assumption that the magnetic field is a tilted dipole.

The first step consists in obtaining a reasonable fit to our 23 LSD Stokes I profiles. Synthetic Stokes I profiles are calculated using an Atlas9 LTE model atmosphere with effective temperature and surface gravity corresponding to those determined for β Cep. First we determine a model local profile, characterised by Landé factor $z = 1.25$ (equal to the mean Landé factor of the LSD profiles) and (assumed Gaussian) turbulent broadening (of Doppler width W). The depth of this profile is adjusted so that, when integrated over the stellar disc, the resultant profile has the same equivalent width as the observed profiles of β Cep. We then add up the Doppler-shifted limb-darkened local profile contributions from all over the stellar surface, assuming a line-of-sight projected rotation velocity $v\sin i$ and fundamental mode radial pulsation (according to the pulsation period of Pigulski & Boratyn 1992) with a velocity amplitude $v_{\rm p}$. We finally convolve the resulting synthetic line by

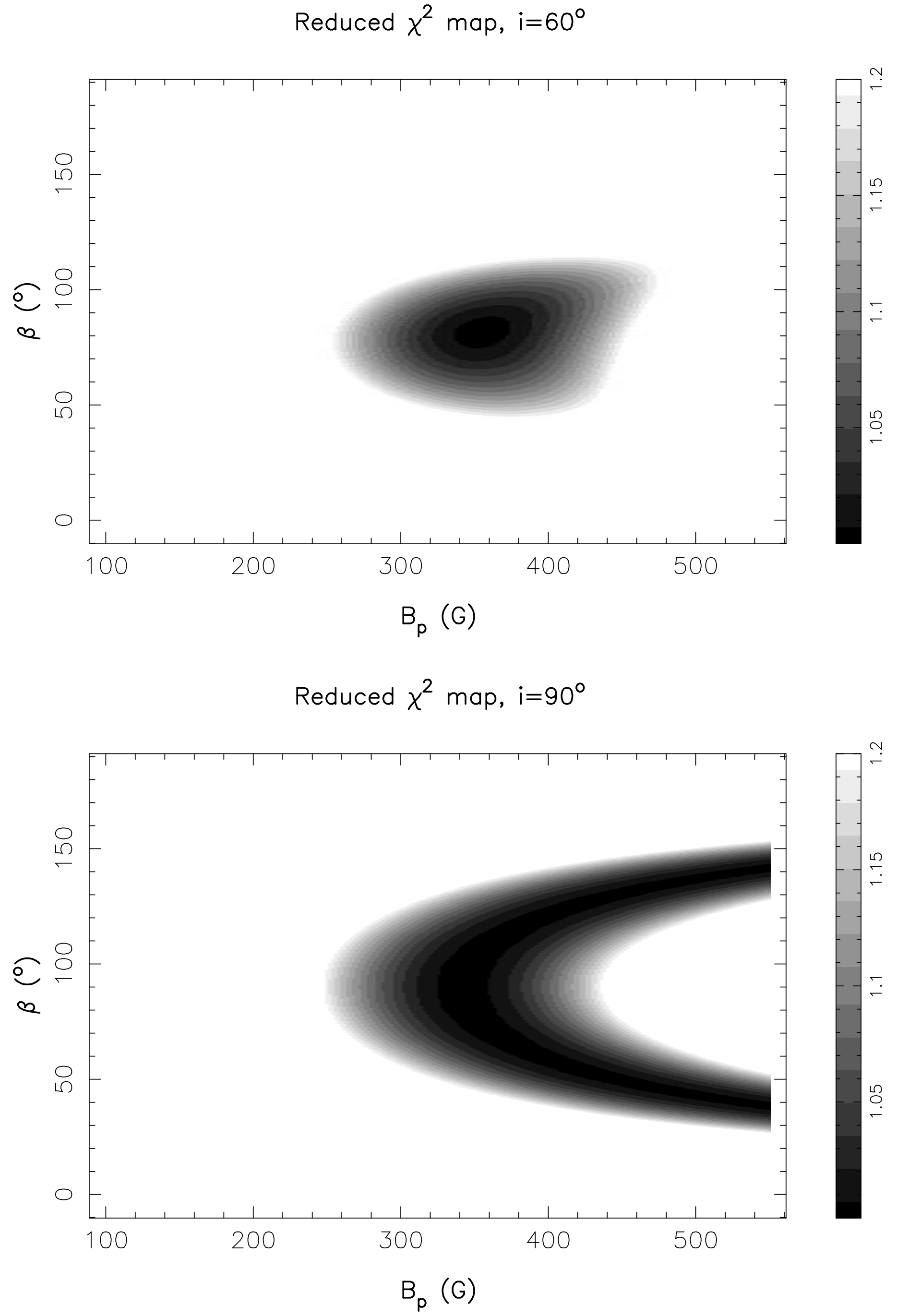

Figure 3. Reduced χ^2 (normalised to the minimum map value of 0.80) as a function of the magnetic dipole model parameters $B_{\rm p}$ and β, for an assumed inclination angle i of 60° (upper panel) and 90° (lower panel). The 68% (1σ) and 99% confidence thresholds correspond to reduced χ^2 increases of 3% and 20% respectively.

an (assumed Gaussian) instrumental profile corresponding to a spectral resolution of 35,000. We point out that β Cep exhibits substantial broadening of its spectral lines which cannot be directly attributed to thermal, pulsational or rotational effects, and which we model as turbulence. Although the origin of this broadening is not known, it seems to be a common feature in spectra of O and B stars (Howarth et al. 1997).

The best fits to the Stokes I profiles obtained by varying the 3 model free parameters (i.e. $v\sin i$, $v_{\rm p}$ and W) are reached for $v\sin i$ values of 28 ± 2 km s^{-1} and correspond to reduced χ^2 of about 3 (sufficient for our ultimate purpose of modelling Stokes V profiles, see next paragraph). Unsurprisingly, we note some degeneracy between $v\sin i$ and W, implying that both parameters cannot be determined independently. Choosing $v\sin i = 27$ km s^{-1} (to remain fully consistent with the conclusions of Sect. 2.1), we obtain a turbulent broadening width of $W = 18\pm2$ km s^{-1} and a pulsation velocity amplitude of $v_{\rm p} = 21\pm1$ km s^{-1}, in good agreement with the results of Telting et al. (1997).

In a second step, we use the derived model parameters $v \sin i$, $v_{\rm p}$ and W to synthesise series of model LSD Stokes V profiles (assuming a Landé factor and central wavelength of 1.25 and 510 nm respectively) for various values of $B_{\rm p}$ and β, that we then compare to the observed ones by computing the corresponding reduced χ^2. The resulting χ^2 maps (shown on Fig. 3) indicate that the most likely polar field strength and magnetic dipole tilt are respectively equal to 355 ± 40 G and $80° \pm 15°$ if the inclination angle is $60°$. Once again, $B_{\rm p}$ and β become more and more correlated as i is increased, and can no longer be disentangled when i reaches the (less probable) value of $90°$, being only constrained by $B_{\rm p} \sin \beta = 340 \pm 40$ G. In both cases, the solutions correspond to a reduced χ^2 of 0.8, demonstrating that the Stokes V data are fitted right down to the noise level. The best fit to the LSD profiles is shown on Fig. 1. As with the previous method, the Stokes V data are still too noisy to identify reliably potential departures from a pure dipolar geometry. These results are in good agreement with those obtained in Sect. 3.2.

4 THE MAGNETICALLY CONFINED WIND OF β Cep

Although one of the weakest detected to date on a stellar surface, the magnetic field of β Cep is nevertheless expected to affect dramatically the stellar radiatively-driven wind. The fact that maximum C IV absorption occurs when the magnetic equator appears edge-on to the observer (i.e. at phases 0.25 and 0.75), as in many magnetic He peculiar stars (Shore & Brown 1990), strongly argues for density enhancements trapped within the magnetospheric equator and forced to corotate with the star (see also Smith & Groote 2001). It demonstrates at the same time that the usual picture describing strong C IV absorption as a tracer of mass outflow in hot stars (e.g. Stahl et al. 1996) is probably not adequate, at least in the case of magnetic stars.

One aim of the present study is to see whether the theoretical models of magnetic wind confinement can quantitatively reproduce all observational constraints.

4.1 The magnetically confined wind shock model

The most detailed and recent theoretical study describing how a dipolar magnetic field affects the radiatively-driven wind of an early-type star is that of Babel & Montmerle (1997a). In their model (called magnetically-confined wind shock model or MCWS, and inspired from earlier work by Havnes & Goertz 1984), a dipolar magnetic field confines and directs the stellar wind from both magnetic hemispheres towards the magnetic equatorial plane, where their collision produces a strong shock. While this shock originally occurs in the magnetic equatorial plane, material accumulation forces it to recede towards the stellar surface until the postshock region is sufficiently extended so as to allow dissipation of the energy deposited by the wind (and thus reach a steady state). The resulting circumstellar structure following the shock consists of an extended high-temperature, low-density postshock region (where X-rays are produced very efficiently) and a geometrically thin, low-temperature, high-density "cooling disc" located in the magnetic equatorial plane (Babel & Montmerle 1997a). Although originally developed to explain the X-ray emission of the Ap star IQ Aur, MCWS has been applied for the same purpose to the young O7 star θ^1 Ori C (Babel & Montmerle 1997b), suggesting that its applicability is probably much broader than originally thought. For more information about the detailed physics underlying the MCWS model, we refer to the original work of Babel & Montmerle (1997a).

We have produced a wind shock model specific to the case of β Cep, with a wind structure scaled up from that obtained by Babel & Montmerle (1997a) for IQ Aur using the wind parameters determined in Sect. 2.1. This model is very similar to model #4 of Babel & Montmerle (1997a, see their Table 3), except for the strength of the magnetic dipole and thus the associated X-ray luminosity and temperature. The structure of the magnetosphere is however not affected within the region where the field is large enough to ensure magnetic confinement of the wind (i.e. magnetic energy larger than wind kinetic energy). Our new model indicates that the field is strong enough to confine the wind all the way to the magnetic equator (prior to the initial shock) up to a distance of about 8 R_* (corresponding to a magnetic colatitude of field line footpoints of 21°). Along the magnetic axis itself, the wind is confined even further, up to a distance of roughly 9 R_*.

We determined the structure and physical properties of the magnetosphere for this particular model. The temperature structure in the postshock region that we obtain is depicted in Fig. 4. The position of the shock (once stationary) is very similar to that of model #4 (see Fig. 13 of Babel & Montmerle 1997a), and we find that the wind ram pressure just before the shock decreases from 0.31 to 0.077 $\mathrm{g\,cm^{-1}\,s^{-2}}$ for respective magnetic colatitudes of field line footpoints ranging from 45° to 20°. The total (i.e. thermal plus ram) pressure in the postshock region, equal to the pre-shock wind ram pressure at the shock front, progressively decreases along the field lines towards the magnetic equator (to compensate for the postshock region gravitational pressure), reaching a value that only varies from about 0.15 $\mathrm{g\,cm^{-1}\,s^{-2}}$ at a radial distance of 2 R_* (magnetic colatitude of field line footpoint of 45°) down to 0.045 $\mathrm{g\,cm^{-1}\,s^{-2}}$ at 8.5 R_* (magnetic colatitude of field line footpoint of 20°). We finally obtain that the density $\rho_{\rm D}$ of the cooling disc (whose temperature is assumed to decrease outwards from 15000 K to 10000 K, Smith & Groote 2001) is roughly constant in this distance range, and equal to about 5×10^{-14} $\mathrm{g\,cm^{-3}}$ or 3×10^{-10} $\mathrm{cm^{-3}}$. This is in good agreement with the values derived by Smith & Groote (2001) from a detailed modelling of all IUE spectra of β Cep.

4.2 X-ray luminosity and variability of β Cep

To quantify the X-ray emission produced in the postshock region of our β Cep model, we integrate over the whole magnetosphere the local X-ray emissivity computed from MeKaL models (Mewe et al. 1995). We carry out the integration for various angles between the line-of-sight and the magnetic axis, assuming that the wind and postshock region are optically thin at X-ray wavelengths. We find that the X-ray spectrum produced by our model can be well-fitted in the energy range 0.1–2 keV with a luminosity, temperature and emission measure of 7.2×10^{30} $\mathrm{erg\,s^{-1}}$, 3.2 MK and 4.5×10^{53} $\mathrm{cm^{-3}}$, in very good agreement

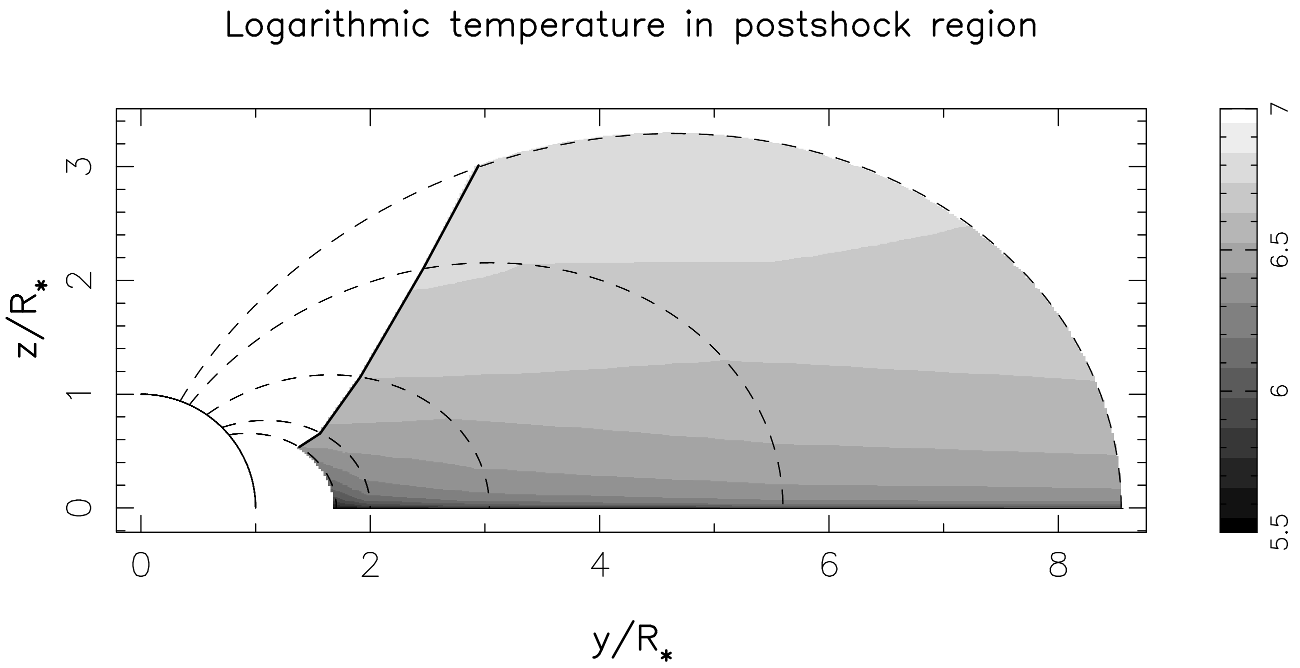

Figure 4. Logarithmic temperature in the postshock region for our magnetically-confined wind shock model of β Cep. The thick line depicts the location of the shock, while the dashed ones illustrate the field lines corresponding to footpoint colatitudes of 50°, 45°, 35°, 25° and 20°.

with the β Cep ROSAT measurements (respectively equal to $5-10\times10^{30}$ erg s^{-1}, 2.8 MK and $2-5\times10^{53}$ cm^{-3}, see Sect. 2.1). We also find that the predicted X-ray radiation of β Cep is significantly more intense than that of the isothermal model at higher energies. It confirms that the magnetically-confined wind shock model is perfectly capable of explaining quantitatively the X-ray emission of β Cep, and thus appears much more appropriate than the self-excited wind instability mechanism usually invoked for hot stars (e.g. Cohen et al. 2001).

We also expect the X-ray flux we observe from β Cep to be modulated periodically under the effect of several competing factors, as the star rotates and the oblique postshock region changes its orientation with respect to the observer. First, the central star occults a variable fraction of the X-ray emitting postshock region (maximum occultation occurring when the disc is seen edge on). Given the large size of the postshock region, we obtain that this effect is marginal and only modulates the X-ray light curve by less than 10%. Secondly, X-rays are absorbed by cool material along the line-of-sight, either the cool wind or the cooling disc (maximum absorption occurring when the disc is perpendicular to the line of sight). While the cool wind is almost completely transparent for a mass loss rate as low as that of β Cep (e.g. Cohen et al. 1997), the high density cooling disc is totally opaque and masks most of the X-ray flux emitted by the hidden magnetic hemisphere except when the disc is seen close to edge on, allowing both hemispheres to be visible to the observer. In principle, we therefore expect the X-ray light curve of β Cep to feature essentially two sharp peaks centred at phases 0.25 and 0.75. This result depends however very much on the actual shape of the cooling disc; if for instance the disc gets thick enough or warped at large distances, it may occult some of the postshock region when seen edge on, thereby strongly affecting the detailed shape of the X-ray light curve. We therefore only conclude that the phase and amplitude of the X-ray rotational modulation remain essentially matters of speculation.

The recent discovery that the X-ray flux of β Cep varies periodically with the radial pulsation phase (Cohen et al. 2001) is also interesting and potentially very instructive in the context of the magnetically-confined wind shock model. As mentioned already in Sect. 2.1, the impact of the radial pulsation on the wind is, at first order, to modulate the mass-loss rate by about ±20%. In the framework of our model, the pulsation is expected to modulate the whole shock and postshock region. By computing a new magnetospheric model with 20% stronger mass loss, we find that the shock moves slightly towards the equator when the wind is stronger, increasing at the same time (by about 5%) the wind velocity just before the shock front. Altogether, we obtain that the local X-ray luminosity of the postshock region is enhanced by about 30%, and that the time for the postshock region to reach a new equilibrium is of the order of the time for an Alfven wave to reach the magnetic equator. It implies that the postshock region settles more rapidly than half the pulsation period only for field lines with footpoint colatitudes larger than 35° (intersecting the magnetic equator at about 3 R_*). We thus make the simplifying assumption that the local X-ray luminosity fluctuates by ±30% within this region, and remains constant outside. Note that the time for the stronger wind to reach the shock is longer for longer field lines, implying that all points of the shock and postshock region do not oscillate in phase. Taking into account this phase difference and integrating over the postshock region, we find that the global X-ray luminosity fluctuates by about 5%, in reasonable agreement with the observed value of 6.7% (Cohen et al. 2001). We also obtain that the delay between the epochs of maximum visible brightness and maximum X-ray luminosity corresponds to a phase shift of about 1.13 pulsation cycles. From Cohen et al. (2001), we can estimate that β Cep reached maximum X-ray flux at JD $= 2,448,861.05 \pm 0.01$; from the spectroscopic observations of Telting et al. (1997, obtained only 3 months earlier than the ROSAT run of Cohen et al. 2001), we infer that β Cep reached maximum radial velocity at JD $= 2,448,758.50$, and thus also at JD $= 2,448,860.98$ (using a fundamental radial pulsation period of 0.1904852 d, Pigulski & Boratyn 1992). We thus conclude that the time delay between maximum light (occurring 0.267 pulsation cycles or 0.05 d later that maximum velocity, Pigulski & Boratyn 1992) and maximum X-ray flux is 0.02 ± 0.01 d or 0.10 ± 0.05 pulsation cycles, in perfect agreement with the predictions of our magnetospheric model (given the fact that this delay can only be estimated to within an integral number of pulsation cycles). Our model is thus very successful at explaining all available X-ray observations of β Cep.

5 DISC INSTABILITIES: AN EXPLANATION OF THE BE EPISODES?

Another important challenge for any model aimed at describing the magnetospheric environment of β Cep is to explain as quantitatively as possible the recurrent Be episodes, i.e. the phases of hydrogen-emission that β Cep undergoes every few decades (Mathias et al. 1991, Pan'ko & Tarasov 1997). It may also provide at the same time some interesting insights into the Be phenomenon in general, whose detailed physical mechanisms are still very poorly understood. The case of β Cep is particularly interesting in the sense that it is not a rapid rotator (unlike the vast majority of Be stars), implying that rapid rotation per se is not the universal cause of the Be phenomena, in contradiction with what is often stated in the literature. Several tentative explanations of β Cep's Be episodes have already been suggested in the literature, but they are not entirely satisfactory. For example, Kaper & Mathias (1995) suggested a possible variation of the magnetic field topology, which now seems extremely unlikely given the fossil-like magnetic field we inferred.

By examining the stability of the MCWS model described in Sect. 4 on a time scale of years to decades, we can provide new clues regarding the source of the Be phenomenon of β Cep. For simplicity, we consider in the following that the magnetic and rotation axes of β Cep are orthogonal (i.e. $\beta = 90°$), and thus that the magnetic equator contains the rotation axis. The main source of instability in our magnetospheric model can be found in the high density cooling disc itself. Being forced to corotate with the field, the ionised disc plasma (whose temperature ranges between 10000 and 15000 K) experiences a non-zero local effective gravity $g_{\rm eff}$ (defined as the gravitation plus centrifugal acceleration), except at two points (called corotation points in the following and located 7.2 R_* away from the centre of the star, at the intersection of the magnetic and rotation equator). Note that the particular magnetic geometry of β Cep (with the rotation axis included in the magnetic equator) is responsible for the fact that the effective gravity field within the magnetic equator is not symmetric with respect to the centre of the star.

Two different types of instabilities, described in the following paragraphs, can develop in the disc, depending essentially on the strength of the local magnetic field and the direction of the local effective gravity. If the field is strong enough and the effective gravity is pointing inwards, the weight of the disc plasma is transfered back onto the wind along field lines, eventually quenching it momentarily; if not, field lines get distorted to attempt resisting the effective gravitational force.

5.1 Quenching the wind

Being sandwiched between the postshock regions of both hemispheres, the disc plasma cannot spontaneously flow back to the stellar surface, even when $g_{\rm eff}$ is directed inwards. Therefore, as it is being filled by the wind, the disc progressively thickens at roughly constant pressure and thus constant density. It is only when the gravitational pressure of the disc along field lines (equal to about $0.25\rho_{\rm D}g^{\rm r}_{\rm eff}{h_{\rm D}}^2/r$ where $h_{\rm D}$ is the disc height and $g^{\rm r}_{\rm eff}$ the radial component of $g_{\rm eff}$) exceeds the pressure of the postshock region, that the wind is momentarily stopped and the disc plasma flows back toward the star (as described by Babel & Montmerle 1997a). Estimating $h_{\rm D}$ from:

$$\rho_{\rm D}h_{\rm D} = \frac{J\Delta t}{L^3}\left(1-\frac{1}{L}\right)^{-1/2} \tag{1}$$

where J is the mass flux per unit area at the stellar surface (taken from Fig. 5 of Babel & Montmerle 1997a and multiplied by 20 to account for the larger mass loss rate of β Cep), Δt the time elapsed since the matter has begun to accumulate in the magnetic equator and L the magnetic shell parameter (equal to r/R_* within the magnetic equator), we find that the disc filling time before the plasma starts to flow back increases strongly outwards from 0.1 yr at $L = 3$ to 1 yr and over for $L > 5$.

As mentioned above, this scenario can only occur if the effective gravity is pointing inwards and if the local magnetic field is strong enough to support the disc plasma until its gravitational pressure along field lines reaches the pressure of the postshock region. To investigate whether this is the case, we estimate the magnetic tension of field lines (equal to ${B_{\rm e}}^2/4\pi r_{\rm c}$ where $B_{\rm e} = 0.5B_{\rm p}/L^3$ is the local field strength in the magnetic equator and $r_{\rm c}$ the curvature radius of field lines) by assuming that $r_{\rm c}$ is of the order of the disc thickness $h_{\rm D}$. We thus consider that the above condition is verified if the local field obeys:

$${B_{\rm e}}^2 \geq 4\pi\rho_{\rm D}h_{\rm D}g_{\rm eff} \tag{2}$$

when the disc filling time is reached. We find that this condition is fulfilled only in the inner disc, for $L < 3$. In the outer disc, the right-hand side of the expression very quickly dominates the left-hand side, by as much as 2 orders of magnitude around $L = 6$.

We therefore conclude that in the inner regions, the disc should empty itself very frequently, by leaking along field lines and momentarily quenching the wind. The associated energy release is expected to be quasi-continuous and thus does not contribute to the episodic Be events.

5.2 Stretching the field lines

In the outer disc, the field is not strong enough to support the plasma until the disc filling time is reached; field lines should thus become significantly stretched in attempting to resist the gravitational collapse of the disc plasma. To estimate how, how much and how fast field lines are distorted, we use the following very simple model. Note that this model only aims at exploring the longer-term evolution of the disc and does not pretend to be as accurate and self-consistent as a full MHD study (that we postpone for the future). Consider a local bubble of plasma within the magnetic equator, whose mass increases steadily with time as described by Eq. 1. The main forces acting on this bubble of plasma are (in a non rotating frame) the gravitational force, the magnetic tension of field lines (opposed to the displacement of the bubble in the corotating frame) and a viscous force of arbitrary nature (proportional and opposed to the velocity of the bubble in the corotating frame) to damp rapidly potential oscillatory behaviour. The role of this viscous force is to model very roughly the interaction of this plasma bubble with the rest of the disc and magnetic structure, that we do not explicitely take into account here. Note as well that, given the high density and small velocity dispersion in the disc, the radiative force only plays a significant role in the very inner disc regions and is thus ignored in our simple model.

We use the same criterion as above (see Eq. 2) to determine the time during which the field can hold the disc weight. We obtain that this time decreases outwards (except around the two corotation points), from about 0.1 yr at $L = 3$ down to less than 0.02 yr for $L > 8$. Since $h_{\rm D}$ increases linearly with time in this interval, we can also derive the maximum thickness the disc reaches, equal to ${B_{\rm e}}^2/4\pi\rho_{\rm D}g_{\rm eff}$ after Eq. 2. We then assume that, when this limit is attained, the portion of field lines crossing the cooling disc is stretched for the magnetic tension to compensate the effective gravitational force. We further assume in this simple model that, once its maximum value is reached, $h_{\rm D}$ remains constant while $\rho_{\rm D}$ increases linearly with time (following again Eq. 1).

The dynamical evolution of the plasma bubble during the latter phase is estimated by integrating numerically the equation of motion on the required timescale. Note that although all forces are contained in the magnetic equatorial plane, the simple fact that this plane rotates about an axis included in this plane (the rotation axis) implies that the plasma can potentially move out of the plane (under the effect of the Coriolis force if we now consider the corotating frame). However, we find that field lines are eventually only elongated, in the corotating frame, along the local vector field of effective gravity, and that all plasma motions perpendicular to the magnetic equator are rapidly damped by the viscous force we invoked. The elongation of field lines can thus be described with an equation similar to Eq. 2:

$$B^2 = 4\pi\rho_{\rm D}h_{\rm D}g_{\rm eff} \qquad (3)$$

where B is the magnetic strength along the stretched field lines.

As the wind continues to fill the disc, field lines become increasingly distorted, building up a strong field gradient across the cooling disc and hence a current sheet in the magnetospheric equator. The approximate displacement of the fluid bubble (from its original position just after the shock) and the associated magnetic field gradient 10 yr after the initial shock are illustrated on Fig. 5, for radii ranging between 3 and 8.5 R_*. The departure from axial symmetry (about the magnetic axis) is of course due to the particular magnetic geometry of β Cep, whose rotation axis is included in the magnetic equator. It is important to realise that even a small displacement of plasma can produce a large magnetic amplification, the relevant parameter being the ratio of the local plasma drift to the local disc thickness. The fact that $h_{\rm D}$ decreases outwards (except around the corotation points) faster than the plasma displacement explains in particular why both field elongation and magnetic gradient increase outwards. Similarly, at given L, smaller plasma drifts are observed where the effective gravity (and thus magnetic amplification) is stronger (i.e. along the rotation axis); this is due to the fact that $h_{\rm D}$ also varies with (and more precisely in inverse proportion to) the local effective gravity, thereby allowing larger field amplifications to be achieved with smaller plasma displacements.

5.3 Reconnection of distorted field lines

To investigate whether such instabilities may be invoked to explain the Be phenomenon of β Cep, we must check that the associated timescale is of the same order of magnitude than the recurrence period of Be episodes. To estimate the typical timescale τ for the current sheet that developed in the magnetic equator to tear, and thus the distorted field to reconnect by resistive diffusion, we use the following expression (Mestel 1999):

$$\tau = (\tau_{\rm A}\tau_{\rm d})^{1/2}$$

where $\tau_{\rm A}$ and $\tau_{\rm d}$ are respectively the Alfven and diffusion times across the disc. Note that this timescale does not change much as the disc fills up, $\tau_{\rm d}$ being only very weakly sensitive to $\rho_{\rm D}$ (through the Coulomb logarithm) and $\tau_{\rm A}$ remaining constant when B increases as ${\rho_{\rm D}}^{1/2}$ (see Eq. 3). As shown in Fig. 6, this timescale varies from 1 yr in the outer disc regions, up to 100 yr around $L = 3$ and the corotating points.

From Fig. 5 we see that the cooling disc can be divided into two distinct regions. Within the dashed line, reconnection starts far above the rotation equator and slowly propagates toward the rotation equator, then toward the star, as plasma released by reconnecting field lines is transferred to smaller radii. We obtain that 30 yr after the initial shock, the mass deposited in the outer disc regions (between $L = 4.5$ and the dashed line, i.e. about half the total disc mass) has been transfered to the inner disc ($L < 4.5$), further increasing (by about 40%) the field distortion in these regions with respect to the predictions of Fig. 5 (once scaled up by a factor of 1.7 to account for the longer time span). This implies in particular that most of the mass deposited in the disc within the dashed limit and within 30 yr of the initial shock should be hanging in field lines within only 1 R_* of the stellar surface, thus showing that the time for the disc to fill up and collapse (i.e. to complete a full cycle) cannot be much longer than 30 yr. We emphasise again that our modelling is very rough, and cannot describe in particular the final phase of this process; we suggest that it shares some

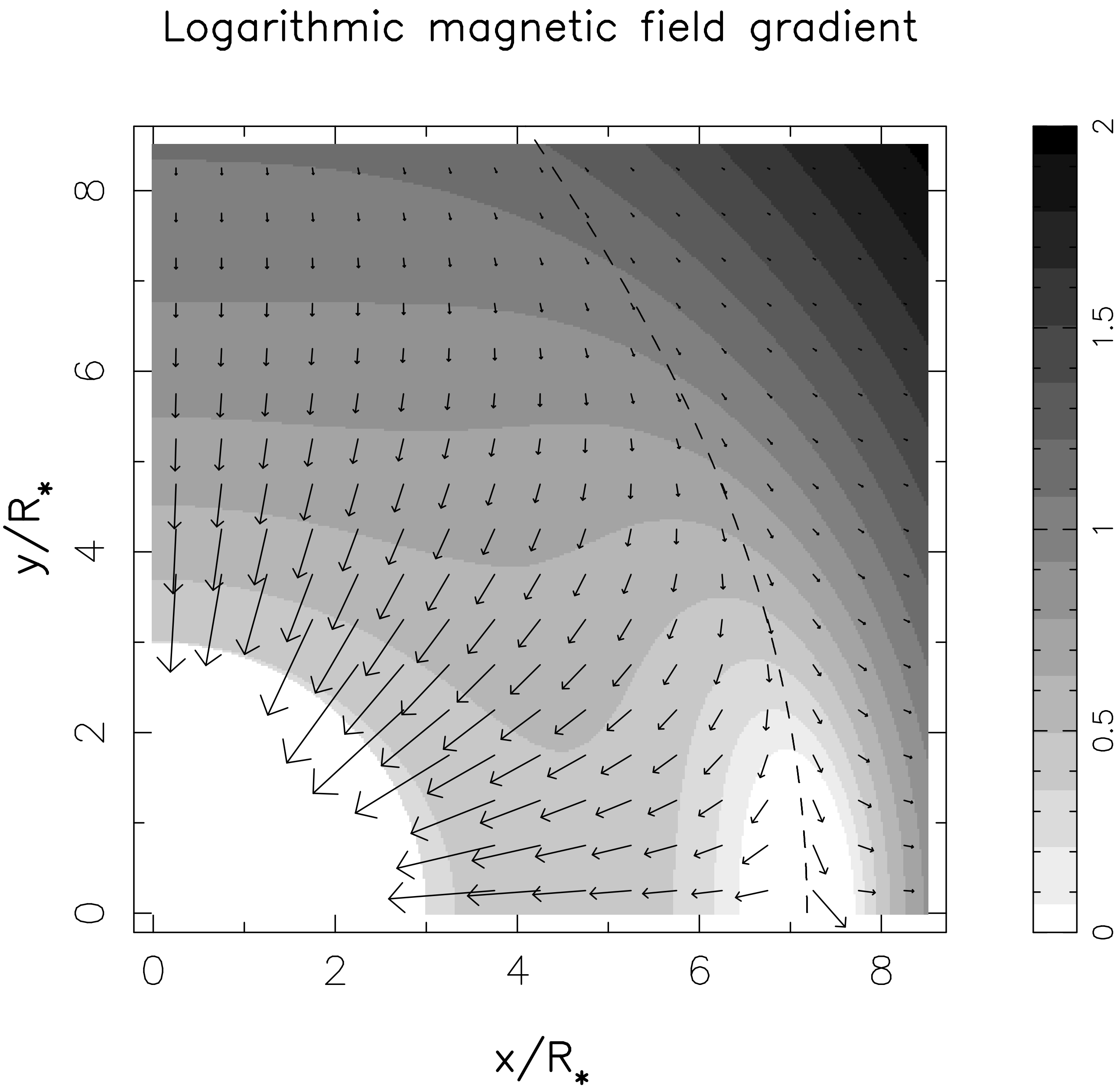

Figure 5. Logarithmic magnetic field gradient (in units of $B_{\rm p}/R_*$, grey scale) across the cooling disc and associated displacement of plasma (from its original position just after the shock, arrows) 10 yr after the occurrence of the shock, and for radii ranging between 3 and 8.5 R_*. Note that the graph only shows one quadrant of the magnetic equator (viewed from the magnetic axis), with the y and x axes depicting respectively the rotation axis and the intersection between the magnetic and rotation equators. The local minimum in field gradient located at $(x,y) = (7.2\ R_*,0)$ corresponds to one corotation point. The dashed line separates the region where material collapses towards the star (on the left-hand side) from that where plasma is ejected away from the star (on the right hand side).

similarities with eruptive phenomena on the Sun where an exceedingly stressed magnetic field quickly returns to a potential configuration through fast reconnection. We model this very schematically by considering that the reconnection timescale inwards of $L = 4.5$ is equal to 30 yr.

Given the fact that the recurrence timescale of the Be phases of β Cep, of the order of a few decades, is compatible with the estimated time to empty the regions of the cooling disc within the dashed limit (of the order of 30 yr), we suggest that these events may be related to the final (eruptive) phases of the reconnection phenomena described in the previous paragraph. We must however caution that this agreement may be somewhat fortuitous (given the additional fact that our understanding of reconnection physics is still approximate) and that our results must be confirmed through more sophisticated models.

The reconnection induced energy release during these 30 yr is expected to be strongly time-dependent. While reconnection in the outer disc regions is frequent, it is only weakly energetic. Reconnection in the inner disc, on the other hand, dissipates considerably more energy but occurs only every few decades; lowest temporal frequencies should

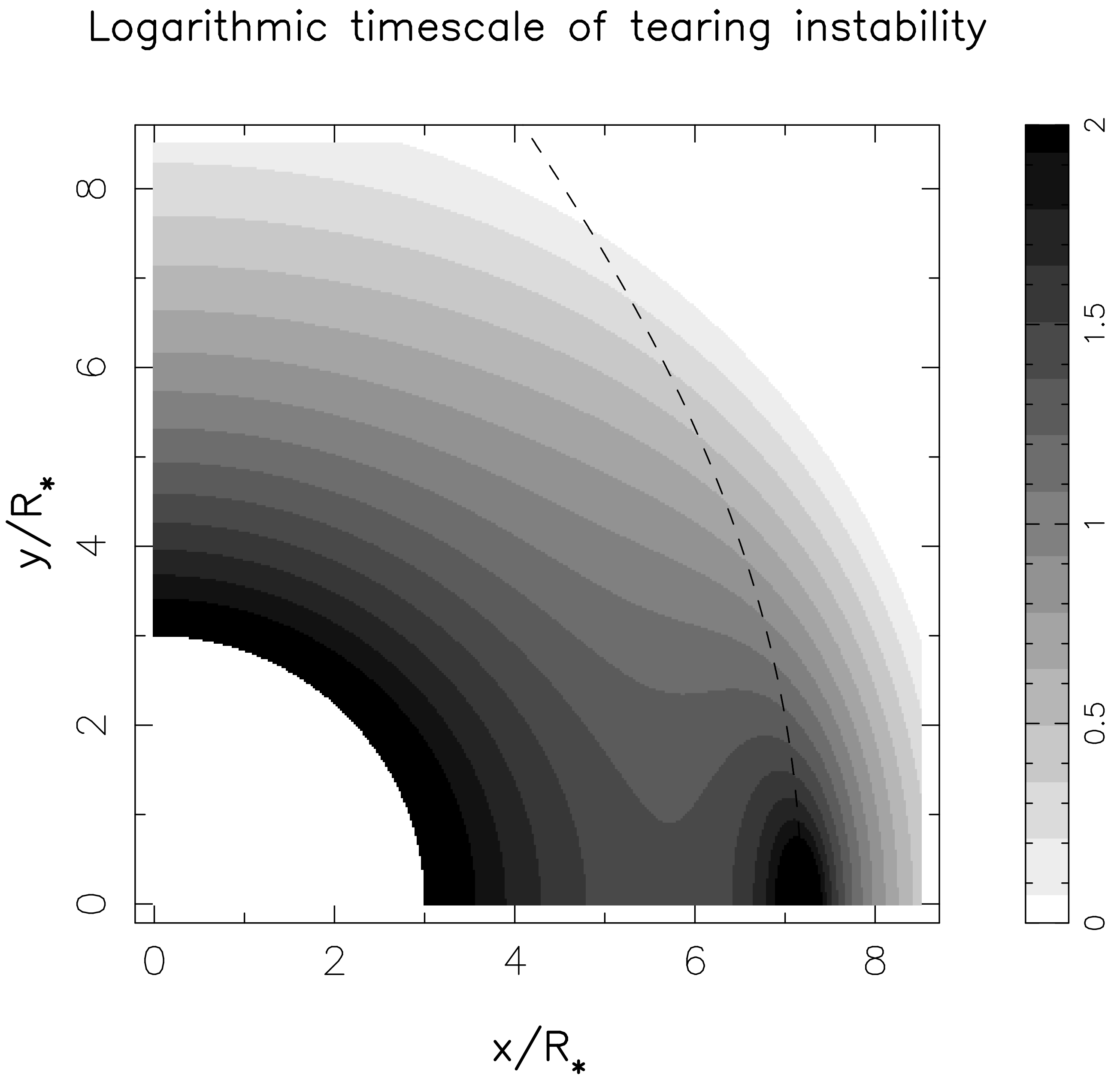

Figure 6. Logarithmic timescale (in yr) for the tearing mode instability to develop in the disc and produce field reconnection, for radii ranging between 3 and 8.5 R_*. See Fig. 5 for the meaning of all graphics symbols.

therefore largely dominate the resulting luminosity curve. Outside of the dashed limit, the timescale of the tearing instability is much shorter, generally shorter than one year; this implies that the associated plasma is almost continously expelled away from the star by the centrifugal force (without triggering in particular a chain reaction as in the previous case) and that the associated (very weak) energy release is roughly time-independent.

Using our simple model, we can estimate the rate of magnetic energy release during the Be phases by assuming that the stressed field topology returns to its original configuration; we obtain a peak value of about $5 \times 10^{-8}\ L_{\rm bol}$. Note that this estimate is only a lower limit, as some of the potential and kinetic energy stored in the inner disc may also very likely be dissipated (at a maximum rate of about $5 \times 10^{-6}\ L_{\rm bol}$) when the disc plasma is dumped back onto the stellar surface. Reconnection processes taking place in the outer disc regions (outside the dashed limit of Fig. 5) and including no more than a few percent of the total disc energy, are believed to occur steadily (rather than episodically) and should therefore contribute only very marginally to the Be episodes of β Cep.

While actual measurements of the amount of energy released during a typical Be episode of β Cep are not yet available in the literature for comparison with our predictions, it should be possible to estimate it during the next such event through multi-wavelength observations. Worth mentioning in this respect is the result of Henrichs et al. (2001) that the rotational modulation observed in UV resonance lines (interpreted as recurrent occultations of the central star by the rotating cooling disc) did not change between the two main IUE observing epochs (1979 and 1992–1995) and in particular within (1992–1993 data) and without (1979 data) a Be episode. This is further confirmed by Smith & Groote (2001) who could demonstrate that the disc contribution to the total column density towards β Cep (of order 10^{23} cm^{-2}) did not vary much (less than a factor of 10, Smith private communication) between the two epochs. This could indicate a potential discrepancy with our model, which predicts that the amount of absorbing plasma within the inner disc should increase with time between two successive Be episodes (with densities raising from about 3×10^{10} cm^{-3} after a massive reconnection event up to about 3×10^{12} cm^{-3} before the next event).

6 DISCUSSION

One way to test our model further is to check whether it is compatible, at least to first order, with the phenomenology observed to be associated with similar stellar classes. In the following paragraphs, we assume that our β Cep model applies to other stars (of similar mass, radius and temperature as β Cep), check for potential incompatibilities, and derive, whenever possible, basic constraints the observations impose on the main model parameters.

If β Cep shares obvious similarities with He peculiar stars (as recalled several times in this paper already), one should nevertheless note that two important differences exist; while β Cep does not feature any strong abundance anomalies (Gies & Lambert 1992), He peculiar stars have never been reported yet as undergoing Be phenomena. The absence of abundance anomalies in β Cep is not really surprising: diffusion can simply not compete with a mass loss rate as strong as 10^{-9} $M_{\odot}\,\mathrm{yr}^{-1}$. This agrees in particular with the observation that all He peculiar stars are significantly cooler than β Cep and thus lose mass at a much smaller pace. Moreover, with a magnetic field stronger than that of β Cep by typically one to two orders of magnitude, He peculiar stars should feature field lines that can resist elongation at least 100 times longer than those of β Cep (all other parameters being equal), implying that their disc plasma flows back to the star along field lines before it starts distorting the magnetic field. It therefore implies that He peculiar stars should not undergo Be phenomena similar to the eruptive phases of β Cep, in agreement with observations.

Another class of stars to which β Cep is linked is of course the classical Be stars. As already noted by Babel & Montmerle (1997a), the MCWS model (and thus our own adaptation to the particular case of β Cep) shares clear similarities (and in particular the cool high density disc) with the circumstellar environments of classical Be stars. The main difference between β Cep and a classical Be star is the much larger rotation rate (by typically a factor of 10), and the larger product of mass loss rate and terminal velocity (once again by about an order of magnitude, Prinja 1989) resulting from the lower effective surface gravity of classical Be stars. The additional observation that the X-ray luminosity of Be stars is only marginally stronger than that of β Cep (Cohen et al. 1997) along with the scaling laws of Babel & Montmerle (1997a) suggests that the polar strength of a putative dipole field must be about 100 G. In this context, we obtain that the closed magnetosphere only extends to a diameter of about 2 R_*, with a corotation radius located at 1.5 R_*, and that all magnetic field lines should suffer significant distortion. The first obvious consequence is that most of the disc energy is now located outside the corotation radius, and should be released roughly steadily, at a rate of a few 10^{-6} L_{bol}. Note that this estimate only includes power dissipation from the closed magnetosphere, and that the observed losses could be significantly larger when taking into account the contribution of the open magnetosphere, as described by Babel & Montmerle (1997b). Our model thus predicts that rapidly rotating classical Be stars should be in a permanent state of activity, constantly dissipating energy at a rate higher than that of β Cep during its most active Be episodes. Consider now a Be star with a twice smaller rotation rate (all other stellar parameters kept equal), and whose closed magnetosphere is thus fully included within the corotation radius (located at 2.5 R_*). Our model now indicates that a significant fraction of the energy release should occur during discrete phases, similar to, though much more frequent and energetic than, those of β Cep. Although the details of the process are obviously very much dependent of the exact stellar parameters, the predictions outlined above seem to be in reasonable agreement with observations of classical Be stars. We therefore conclude that our β Cep model may potentially provide new insights toward our understanding of this stellar class. Note that we well recognise that that the detailed physics of circumstellar environments of classical Be stars is very likely much more complex than our simple description, but our present aim is only to demonstrate that there seems to be no basic incompatibility between the MCWS model and the phenomenology observed for this stellar class.

Following these arguments, it is tempting to suggest that the X-ray emission of normal non-supergiant B stars (equally difficult to understand in the framework of the self-excited wind instability mechanism usually invoked for hot stars) is also due to shocks in a magnetically confined stellar wind. The wind parameters of a normal non-supergiant B star with the same spectral type as β Cep are expected to be very similar to those of β Cep. However, the fact that such stars do not exhibit episodic Be episodes (or only very infrequent and/or rather faint ones) would suggest in the context of our model that the cooling disc is much smaller than that of β Cep and thus that the polar strength of the magnetic field is weaker, again around 100 G. The main difference with classical Be stars is the 10 times smaller mass loss rate. In this situation, the unstable disc extends between about 2 R_* (below which the disc plasma flows back to the star along field lines) and slightly less than 4 R_* (above which the wind is no longer magnetically confined). If the star is a rapid rotator like the vast majority of normal non-supergiant B stars (with a rotation rate more than five times larger than that of β Cep), its corotation radius is smaller than 2.5 R_*; it implies that most of the disc plasma is steadily ejected away from the star with a power dissipation smaller than 10^{-7} L_{bol} and that potential Be episodes should be rather dim and very infrequent. According to the scaling laws of Babel & Montmerle (1997a), the associated X-ray luminosity should only be about 2 to 3 times lower than that of β Cep in the case of a closed magnetosphere, again in reasonable agreement with the observations.

A natural question that also comes to mind is whether β Cep was formerly a classical Be star with 10 times larger mass loss and rotation rate, and whose angular momentum was dissipated faster than that of other classical Be stars due to the stronger magnetic field. The magnetic braking timescale $t_{\rm A}$ can be expressed as:

$$t_{\rm A} = k \frac{M_*}{\dot{m}} \left(\frac{R_*}{R_{\rm A}}\right)^2$$

where k is the fractional gyration radius (equal to 0.2 for β Cep, Claret 1995), $R_{\rm A}$ the Alfven radius (about 9 R_* along the open polar magnetic field lines, see Sect. 4) and $\dot{m}$ the effective mass loss rate (determined by only taking into account the material that effectively leaves the star, i.e. associated with field lines intersecting the magnetic equator outside the corotation limit). We obtain $\dot{m} = 2.7\times10^{-10}$ $M_\odot\,{\rm yr}^{-1}$, and thus $t_{\rm A} = 110$ My, an order of magnitude longer than the estimated age of β Cep (see Sect. 2.1). Even if we assume that β Cep was a rapidly rotating Be star with a 10 times larger mass loss rate since the beginning of its life, and take into account the long-term evolution of its radius (according to Schaller et al. 1992), magnetic field (assuming constant flux through the surface), Alfven radius (varying with $B^{2/3}$ at constant mass loss), corotation limit (using Kepler's third law) and $\dot{m}$ (due to the variation of the corotation limit), we still obtain that its rotation period (initially set to 1.2 d) would not exceed 5 d at an age of 12 Myr. We therefore conclude that the rotation braking of β Cep must be due to another mechanism, possibly a strong star-disc interaction in the very early stages of its life (as proposed by Stepien 2000 in the particular case of magnetic chemically peculiar stars). Another (less likely) alternative is simply that β Cep was formed with a much smaller-than-average share of angular momentum.

Finally, yet another test of the model is to check that the continuum linear polarisation (and its rotational modulation) that our model predicts is consistent with actual measurements. A computation with the very recent Monte Carlo stellar wind radiative transfer code of Harries (2000) indicates that the intrinsic continuum linear polarisation of β Cep when the disc reaches its maximum density (3×10^{12} cm^{-3}) should vary from zero (when the disc is seen face on, i.e. at phase 0.0 and 0.5) up to 0.5% (when the disc is seen close to edge on, i.e. near phase 0.25 and 0.75). Continuum linear polarisation measurements by McDavid (9 observations recorded between 1997 Nov. 14 and 1997 Dec. 5, private communication), although showing no definite modulation, suggest that possible phase-locked variations with a full amplitude of 0.06 ± 0.12% are compatible with the data at 68% confidence level. The prediction of our model is thus discrepant with McDavid's observations at a 3.7 σ level, suggesting that the electron density within the disc does not exceed 10^{12} cm^{-3} (assuming that the disc geometry we obtain is correct).

We consider that this disagreement is not (yet) critical given the fact that our model is still very approximate. All assumptions and simplifications made throughout this study could indeed easily produce errors in purely model-dependent quantities such as the disc thickness and electron density (which strongly influence the predicted level of continuum polarisation) by at least a factor of 3, and possibly up to an order of magnitude. More sensitive observations are required for checking our model predictions in more details, not only the actual value of electron density in the disc, but also its possible long-term evolution with time as the cooling disc fills in. This could in particular help us investigate the apparent contradiction of our model with the non-variability of disc parameters suggested by IUE data.

7 CONCLUSIONS

In this paper, we used the very recent spectropolarimetric observations obtained by Henrichs et al. (2001) for the prototypical pulsating star β Cep, to develop for this star a consistent model of the large scale magnetic field and of the associated magnetically confined wind and circumstellar environment.

We redetermined all stellar fundamental parameters from the most reliable studies available in the literature. The value of the rotation period (12.00092 d, Henrichs et al. 2001), along with the most accurate estimates of the line-of-sight projected rotation velocity (27 ± 2 km s^{-1}), distance (182 ± 18 pc) and effective temperature (26000 ± 1000 K) argue strongly in favour of β Cep being a 12 $M_\odot$ star with a radius of about 7 $R_\odot$, viewed at a rotation axis inclination of 60°. Our new estimates of the fundamental parameters of β Cep are consistent with the strongest observed pulsation mode being identified as the fundamental radial mode. They also invalidate the latest conclusions of Shibahashi & Aerts (2000), whose modelling appears not only internally inconsistent (stellar models pulsating on the $\ell = 2$ mode with the second strongest observed frequency seem incorrectly located in the HR diagram) and incomplete (other possible identification of this mode are not discussed), but also incompatible with the observed effective temperature, bolometric luminosity and rotation period.

By using two different modelling strategies, we obtain that the parameters of the magnetic dipole, i.e. the polar field strength $B_{\rm p}$ and the angle between the magnetic and rotation axis β, are respectively equal to 360 ± 30 G and $\beta = 85°\pm10°$ if the inclination angle is about 60°, but cannot be disentangled from one another in the (less probable) case that i reaches 90° ($B_{\rm p}\ \sin\beta = 330\pm30$ G). Our data are still too noisy to allow us to model further the magnetic field, and in particular to identify any potential departure from a purely dipolar configuration.

Although one of the weakest detected to date (and the weakest ever detected in such a hot star), we show that this magnetic field is strong enough to confine magnetically the stellar wind up to a distance of about 8 to 9 R_* (assuming reasonable wind parameters of 10^{-9} $M_\odot\,{\rm yr}^{-1}$ and 900 km s^{-1} for the mass loss rate and terminal velocity respectively). We also show that both the X-ray luminosity and variability of β Cep can be quantitatively reproduced by the magnetically confined wind shock model of Babel & Montmerle (1997a), in which the stellar wind streams from both magnetic hemispheres collide with each other in the magnetic equatorial plane where they produce a strong shock. An extended X-ray emitting postshock region forms under the accumulation of hot (several MK) plasma after the shock front, while a high density cooling disc develops in the magnetic equatorial plane.

By studying the stability of the cooling disc, we obtain that field lines can only sustain the disc for less than a month before they start being significantly elongated to equilibrate the gravitational plus centrifugal force. This elongation of field lines generates a magnetic gradient across the cooling disc, and thus a current sheet that eventually tears, forcing the field to reconnect through resistive diffusion and the associated disc plasma to collapse towards the star. We obtain that, 30 yr after the initial shock, most of the material stored in the cooling disc has accumulated in the immediate vicinity of the stellar surface, and that the associated time-dependent energy dissipation is strongly peaked towards the end of this time interval. We propose that the Be episodes of β Cep are due precisely to this collapse of the cooling disc. We finally suggest that this model could provide new insights in the study of He peculiar, classical Be and normal non-supergiant B stars.

Since our preliminary study indicates that the magnetically confined wind shock seems relevant to the case of β Cep, the next logical step consists of developing a three-dimensional time-dependent MHD simulation of the whole magnetosphere which includes self-consistently the varying mass loss, in order to obtain a proper modelling of the closed and open magnetosphere, of the field line distortion and of the reconnection phenomena in the cooling disc. Such detailed modelling should be able answer whether the Be phenomenon can indeed be explained with the help of magnetically confined winds.

There are also several obvious observational issues. The first goal is to undertake a very high-quality and densely phase sampled linear polarisation monitoring of β Cep (with error bars as small as 0.01%) to validate or invalidate the existence of the circumstellar disc that our model predicts. If detected, this will also allow us to model the physical parameters of the disc, and therefore the whole magnetospheric structure, with much better accuracy. The second goal is to obtain new, more sensitive X-ray observations of β Cep with higher spectral resolution and coverage, using for instance the new X-ray observatory Chandra. Studying individual spectral lines and their time variability should allow us to constrain the temperatures, densities and velocities of the postshock region; moreover, the higher sensitivity of Chandra at shorter wavelengths should help us test our model prediction that the X-ray radiation of β Cep at energies larger than 2 keV is more intense than that predicted by the isothermal model that best fits the ROSAT data. A third issue is to obtain more accurate spectropolarimetric observations of β Cep and to derive a better constrained model of the magnetic field, including in particular higher multipolar terms. Finally, we must also try to detect the magnetic fields of other β Cep stars, as well as those of classical Be stars and normal non-supergiant B stars, to see how generally applicable our model is. The next-generation high resolution spectropolarimeter ESPaDOnS (Donati et al. 1998), currently being built for the Canada-France-Hawaii telescope and whose sensitivity is expected to be much higher than the existing instruments, should be the optimal tool for this exploration.

ACKNOWLEDGEMENTS

This work is based on observations obtained using the MuSiCoS spectropolarimeter and the Télescope Bernard Lyot at Observatoire du Pic du Midi, France. We are very grateful to D. McDavid for communicating linear polarisation data prior to publication. We also thank D. Cohen, M. Jardine, M. Smith and T. Berghöfer for valuable discussion about various points discussed in the paper, as well as John Brown (the referee) for constructive comments on the manuscript. JDJ acknowledges support from the Netherlands Foundation for Research in Astronomy (NFRA) with financial aid from the Netherlands Organisation for Scientific Research (NWO) under project 781-71-053. GAW acknowledges support from the Natural Sciences and Engineering Research Council of Canada (NSERC) in the form of an NSERC postdoctoral fellowship held during the course of this work, and research support from the NSERC operating grants of J.B. Lester and C.T. Bolton (University of Toronto).

REFERENCES

Abbott D.C., 1982, ApJ 259, 282
Babel J., Montmerle T., 1997a, A&A 323, 121
Babel J., Montmerle T., 1997b, ApJ 485, L29
Barker P., Brown D., Bolton C., Landstreet J., 1982, in: Kondo Y., Mead J.M., Chapman R.D. (eds.), "Advances in UV Astronomy". NASA CP–2238, p. 589
Beeckmans F., Burger M., 1977, A&A 61, 815
Berghöfer T.W., Schmitt J.H.M.M., Cassinelli J.P., 1996, A&AS 118, 481
Bessel M.S., Castelli F., Plez B., 1998, A&A 333, 231
Bonneau D., Blazit A., Foy R., Labeyrie A., 1980, A&AS, 42, 185
Claret A., 1995, A&AS 109, 441
Cohen D.H., Cassinelli J.P., Macfarlane J.J., 1997, ApJ 487, 867
Cohen D.H., Finley J.P., Cassinelli J.P., 2001, ApJ (in press)
Donati J.-F., Catala C., Wade G.A., et al., 1999, A&AS 134, 149
Donati J.-F., Catala C., Landstreet J.D., 1998, in: Martin P., Rucinski S. (eds.), "'Fifth CFHT Users' Meeting". p. 50
Donati J.-F., Semel M., Carter B., et al., 1997, MNRAS 291, 658
Fishel D., Sparks W.M., 1972, in: "The Scientific Results From the Orbiting Astronomical Observatory (OAO-2)". NASA SP–310, p. 475
Gies D.R., Lambert D.L., 1992, ApJ 387, 673
Gezari D.Y., Labeyrie A., Stachnik R.V., 1972, ApJ 173, L1
Havnes O., Goertz C.K., 1984, A&A 138, 421
Harries T.J., 2000, MNRAS 315, 722
Henrichs H.F., Bauer F., Hill G.M., et al., 1993, in: Nemec J., Matthews J.M. (eds.), "New Perspectives on Stellar Pulsation and Pulsating Variable Stars". IAU Coll. 139, Cambridge University Press, p. 186
Henrichs H.F., Donati J.-F., Wade G.A., et al., 2001, A&A (submitted)
Henrichs H.F., de Jong J.A., Kaper L., et al., 1998, in: "Proc. UV Astrophysics Beyond the IUE Final Archive", ESA–SP 413, p. 157
Heynderickx D., Waelkens C., Smeyers P., 1994, A&AS 106, 79
Howarth I.D., Siebert K.W., Hussain G.A.J., Prinja R.K., 1997, MNRAS 284, 265
Kaper L., Mathias P., 1995, in: Stobie R.S., Whitelock P.A. (eds.), "Astrophysical Applications of Stellar Pulsation". ASP Conf. Ser. Vol. 83, p. 295
Kurucz R.L., 1993, CDROM # 13 (ATLAS9 atmospheric models) and # 18 (ATLAS9 and SYNTHE routines, spectral line database)

Landstreet J.D., 1982, ApJ 258, 639
Mathias P., Gillet D., Kaper L., 1991, in: Baade D. (ed.), "ESO Workshop Nature and Diagnostics of OB star Variability", p. 193
Mewe R., Kaastra J.S., Liedahl D.A., 1995, Legacy 6, 16
Mestel L., 1999, in: "Stellar magnetism", Oxford University Press.
Pacynski B., 1970, Acta Astron. 20, 47
Pan'ko E.A., Tarasov A.E., 1997, Astron. Lett. 23, 545
Pigulski A., Boratyn D.A., 1992, A&A 253, 178
Preston G.W., 1967, ApJ 150, 547
Prinja R.K., 1989, MNRAS 241, 721
Remie H., Lamers H.J.G.L.M., 1982, A&A 105, 85
Rudy R.J., Kemp J.C., 1978, MNRAS 183, 595
Schaller G., Schaerer D., Meynet G., Maeder A., 1992, A&AS 96, 269
Shibahashi H., Aerts C., 2000, ApJ 531, L143
Shore S.N, Brown D.N., 1990, ApJ 365, 665
Smith M.A., Groote D., 2001, A&A (submitted)
Stahl O., Kaufer A., Rivinius T., et al., 1996, A&A 312, 539
Telting J.H., Aerts C., Mathias P., 1997, A&A 322, 493
Underhill A.B., Divan L., Prevot-Burnichon M.L., Doazan V., 1979, MNRAS 189, 601
Wade G.A., Bohlender D.A., Brown D.N., et al., 1997, A&A 320, 172
Wade G.A., Donati J.-F., Landstreet J.D., Shorlin S.L.S., 2000, MNRAS 313, 851
Zorec J., Briot D., 1991, A&A 245, 150